Journal of Histochemistry & Cytochemistry 59(10) 884–898

DOI: 10.1369/0022155411418115
http://jhc.sagepub.com
SAGE


# Localization of a Wide-Ranging Panel of Antigens in the Rat Retina by Immunohistochemistry: Comparison of Davidson's Solution and Formalin as Fixatives

**Glyn Chidlow, Mark Daymon, John P. M. Wood, and Robert J. Casson**
Ophthalmic Research Laboratories, South Australian Institute of Ophthalmology, Hanson Institute Centre for Neurological Diseases, Adelaide, Australia (GC,MD,JPMW,RJC) and Department of Ophthalmology and Visual Sciences, University of Adelaide, Adelaide, Australia (GC,JPMW,RJC)

## Summary

The preferred fixative for whole eyes is Davidson's solution, which provides optimal tissue preservation while avoiding retinal detachment. Hitherto, the compatibility of Davidson's solution with immunohistochemistry has been largely untested. The goal of the present study was to compare the immunolabeling patterns of a wide-ranging panel of commercially available, previously validated antibodies in formalin- and Davidson's-fixed retinas. Immunohistochemistry was performed in normal pigmented rat eyes and, to facilitate localization of inducible proteins, eyes injected with the bacterial toxin lipopolysaccharide or subjected to laser-induced photoreceptor damage. Specificity of labeling was judged by the morphology and distribution of immunopositive cells, by the absence of signal in appropriate controls, and by comparison with expected staining patterns. Retinas fixed in formalin displayed only adequate morphological integrity but were highly compatible with all 39 antibodies evaluated. Retinas fixed in Davidson's solution displayed morphological integrity superior to those fixed in formalin. Generally, the cellular and subcellular patterns and intensities of immunoreactivities obtained with each fixative were identical; however, Davidson's fixative was less compatible with certain antibodies, such as the neurotransmitter γ-aminobutyric acid, the microglial marker iba1, the macroglial stress protein nestin, and the small heat shock proteins Hsp27 and αB-crystallin, shortfalls that somewhat temper enthusiasm concerning its use. (J Histochem Cytochem 59:884–898, 2011)

## Keywords

immunohistochemistry, retina, Davidson's solution, formalin, rat

Immunohistochemistry has become an indispensable tool in the retina, and indeed the entire central nervous system, by virtue of its specificity, sensitivity, and universality. The technique is exploited by basic scientists to increase understanding of the cellular and molecular architecture of the tissue as well as to provide information relating to the differential expression of molecular markers characteristic of cellular or tissue events of interest. The method is also widely used in other disciplines, for example, by neurotoxicologists for risk assessment of therapeutic compounds (WHO, 2001) and by neuropathologists for diagnosis of disease.

Despite the widespread use of immunohistochemistry in retinal biology, the technique is by no means straightforward. Acquisition of biologically meaningful data requires the use of validated antibodies and an optimized method. Publication of false-negative and false-positive findings is of significant concern in the field of neuroscience (Saper 2005; Rhodes and Trimmer 2006; Fritschy 2008). Key factors to consider are, first, selection of primary antibody, and second, method of fixation/processing. Regarding the former, Rhodes and Trimmer (2006, p. 8017) sound a note of caution: "In many cases commercial antibodies fail even the most fundamental

Received for publication May 26, 2011; accepted June 30, 2011.

**Corresponding Author:**
Glyn Chidlow, Ophthalmic Research Laboratories, Hanson Centre for Neurological Diseases, Frome Rd, Adelaide, SA 5000, Australia
E-mail: glyn.chidlow@health.sa.gov.au

tests of activity and/or specificity." Regarding the latter, fixation and processing largely determine antigenicity. Cryosections are the choice of many researchers but result in poor morphological preservation of the tissue. Formalin-fixed, paraffin-embedded sections offer improved morphology, but artifactual detachment of the retina occurs during processing of the globe and the method is incompatible with some antigens. The preferred fixative for whole eyes is Davidson's solution, which provides optimal tissue morphology while avoiding retinal detachment, attributes that account for its routine use in toxicological assessment of ocular tissues (Heywood and Gopinath 1990; Latendresse et al. 2002; Morawietz et al. 2004; McKay et al. 2009). Taking into account the advantages of Davidson's solution as a fixative for the retina, it is surprising that its compatibility with immunohistochemistry remains largely untested. Indeed, the fixative has been used only occasionally in published work (Chidlow et al. 2005; Kercher et al. 2007). Of particular interest are the results of a recent publication which suggested that Davidson's solution is superior to formalin for retinal immunohistochemistry (McKay et al. 2009).

The goals of the present study were as follows: first, to describe the localization of a wide-ranging panel of immunohistochemical biomarkers, each with high signal-to-background ratios, in the rat retina, and second, to evaluate the compatibility of the fixative Davidson's solution with immunohistochemistry. Key aspects of the study included the use of a standardized protocol; the use of commercially available, previously validated antibodies; and, notably, examination whether fixation in Davidson's solution provided superior results to fixation in formalin. Immunohistochemistry was performed in normal pigmented rat eyes and, to facilitate localization of inducible proteins, in eyes subjected either to laser-induced damage to the photoreceptors or in eyes injected with the bacterial toxin lipopolysaccharide.

## Materials and Methods

### *Animals and Procedures*

This study was approved by the Animal Ethics Committees of the Institute of Medical and Veterinary Science and the University of Adelaide and conforms with the Australian Code of Practice for the Care and Use of Animals for Scientific Purposes, 2004. All experiments conformed to the ARVO Statement for the Use of Animals in Ophthalmic and Vision Research. Adult Dark Agouti rats (approximately 200 g) were housed in a temperature- and humidity-controlled room with a 12-hr light, 12-hr dark cycle and were provided with food and water ad libitum.

For induction of retinal damage via photocoagulation lasering, rats were anaesthetized with an intraperitoneal injection of 100 mg/kg ketamine and 10 mg/kg xylazine. Subsequently, the pupils were dilated by topical application of tropicamide, and approximately 100 spots of a 532-nm continuous wave argon laser with a 10-msec pulse duration were placed on the retina around the optic nerve head avoiding the major vessels. Both eyes of each animal received laser treatment. Rats were killed at 6 hr ($n$ = 3), 1 day ($n$ = 3), 3d ($n$ = 3), and 7 days ($n$ = 3). A further 3 rats served as controls.

For endotoxin-induced retinal inflammation, rats were anaesthetized with isoflurane, and intravitreal injection of 0.2% lipopolysaccharide (LPS; 5 µl in sterile saline) was performed in both eyes after topical application of anesthetic drops. All rats ($n$ = 4) were killed after 6 hr.

### *Tissue Processing and Histology*

All rats were killed by transcardial perfusion with physiological saline under deep anesthesia. Both eyes were enucleated immediately. The left eye of each animal was immersion fixed in 10% buffered formalin for at least 24 hr until processing. The right eye of each animal was immersion-fixed in Davidson's solution for 24 hr and then transferred to 70% ethanol until processing. Davidson's solution comprised 2 parts formaldehyde (37%), 3 parts 100% ethanol, 1 part glacial acetic acid, and 3 parts water (Presnell and Schreibman 1997). Whole eyes were hand-processed according to the following schedule: 70% ethanol for 30 min, 3 × 100% ethanol for 30 min, 2× xylene for 30 min, 50% xylene/50% wax (Surgipath Paraplast, Leica, Peterborough, UK) for 30 min at 62C, 2× wax for 30 min at 62C, embed. Globes were embedded sagittally and 4-µm sections were cut using a rotary microtome. Sections were captured on SuperFrost Ultra Plus slides (Menzel-Gläser, Braunschweig, Germany), blotted, and incubated at 4°C overnight before storage at 37C in the dark.

### *Immunohistochemistry*

Tissue sections were deparaffinized, rinsed in 100% ethanol, and treated for 30 min with 0.5% $H_2O_2$ in absolute methanol to block endogenous peroxidase activity before being taken to PBS. Antigen retrieval of formalin-fixed eyes was achieved by microwaving the sections in 10 mM citrate buffer (pH 6.0) for 10 min at 95–100C. For localization of the extracellular matrix proteins collagen VI and laminin, sections received an additional digestion for 3 min with trypsin (0.25 g/liter) to further unmask antigen sites. To determine the optimal antigen retrieval for Davidson's-fixed eyes, three high-temperature antigen retrieval protocols were tested plus one enzyme antigen retrieval protocol. For the high-temperature methods, sections were microwaved in 10 mM citrate buffer (pH 6.0), 100 mM Tris-HCl buffer (pH 9.0), or 1 mM EDTA buffer (pH 8.0) for 10 min at 95–100C. The microwave used, NEC N702EP, had been previously calibrated such that a stable temperature range of 95–100C was

**Table 1.** Antibodies Used in the Study

| Target | Host | *Clone/Cat No. | Dilution | Source |
|---|---|---|---|---|
| Brn-3 | Goat | sc-6026 | 1:500 | Santa-Cruz |
| Brn3a | Goat | sc-31984 | 1:3000 | Santa-Cruz |
| Calbindin | Mouse | *CB-955 | 1:1000 | Sigma |
| Calretinin | Rabbit | AB5054 | 1:2500 | Millipore |
| CD3 (T cells) | Rabbit | A0452 | 1:3000 | Dako |
| Choline acetyl transferase | Rabbit | AB143 | 1:1500 | Millipore |
| Chx10 | Sheep | AB 9016 | 1:10,000 | Millipore |
| Cyclooxygenase-2 | Rabbit | 160126 | 1:500 | Cayman Chemical |
| Ciliary neurotrophic factor | Goat | AF 557-NA | 1:750 | R&D |
| αB-crystallin | Mouse | *G2JF | 1:1000 | Leica |
| ED1 | Mouse | *ED1 | 1:500 | Serotec |
| Collagen VI | Rabbit | Ab 6588 | 1:1000 | Abcam |
| Fibroblast growth factor-2 | Mouse | *bFM-2 | 1:500 | Upstate |
| γ-Aminobutyric acid | Rabbit | A2052 | 1:20,00 | Sigma |
| Glial fibrillary acidic protein | Rabbit | Z0 334 | 1:40,000 | Dako |
| Glutamine synthetase | Mouse | 610517 | 1:1000 | BD Transduction |
| Heat shock protein-27 | Rabbit | SPA-801 | 1:2500 | Stressgen |
| Heat shock protein-32 | Rabbit | SPA-895 | 1:5000 | Stressgen |
| Heat shock protein-70 | Mouse | *C92F3A-5 | 1:500 | Stressgen |
| Iba1 | Rabbit | 019-19741 | 1:50,000 | WAKO |
| Interleukin-1β | Goat | AF 501 NA | 1:1500 | R&D |
| Interleukin-6 | Goat | AF506 | 1:2000 | R&D |
| Inducible nitric oxide synthase | Rabbit | 610332 | 1:500 | BD Transduction |
| Laminin | Rabbit | AT 2404 | 1:3000 | EY Labs |
| Monocarboxylate transporter-3 | Rabbit | MCT-35 A | 1:750 | Alpha Diagnostic |
| Major histocompatibility complex II | Mouse | *OX-6 | 1:500 | Serotec |
| Myeloperoxidase | Rabbit | A 0398 | 1:120,000 | Dako |
| Nestin | Mouse | *Rat 401 | 1:1000 | BD Transduction |
| Parvalbumin | Mouse | *PARV-19 | 1:2000 | Sigma |
| Proliferating cell nuclear antigen | Mouse | *PC10 | 1:20,000 | Dako |
| Protein gene product 9.5 | Mouse | *31A3 | 1:10,000 | Cedarlane |
| Protein kinase Cα | Mouse | *MC5 | 1:1000 | Abcam |
| RPE-65 | Mouse | *8B11 | 1:3000 | Santa Cruz |
| Rhodopsin | Mouse | *RET-P1 | 1:500 | Abcam |
| Synaptophysin | Rabbit | A0010 | 1:2000 | Dako |
| Tumor necrosis factor-α | Goat | AF-426-PB | 1:500 | R&D |
| $\beta_3$-tubulin | Mouse | *TU-20 | 1:1000 | Millipore |
| Tyrosine hydroxylase | Rabbit | Ab 151 | 1:5000 | Millipore |
| Vimentin | Mouse | *V9 | 1:1000 | Dako |

Sigma-Aldrich, Sydney, NSW, Australia; Santa Cruz Biotechnology, Santa Cruz, CA; Dako, Sydney, NSW, Australia; Millipore, North Ryde, NSW, Australia; Abcam, Cambridge, UK; Stressgen, Victoria, BC, Canada; Serotec, Oxford UK; Wako Chemicals, Osaka, Japan; EY Labs, San Mateo, CA; BD Transduction Laboratories, Lexington, KY; Cedarlane, Burlington, NC; R&D Systems, Abingdon, UK; Alpha Diagnostic, San Antonio, TX; Cayman Chemical, Ann Arbor, MI

Note: Upstate is owned by Millipore

achieved when two preheated plastic containers, each filled with 250 ml of retrieval solution, were microwaved on power setting 2. The enzyme retrieval consisted of incubating sections in proteinase K (Dako, Carpinteria, CA; 20 µg/ml for 5 min at room temperature). Following antigen retrieval, tissue sections were then blocked in PBS containing 3% normal horse serum and incubated overnight at room temperature in primary antibody (containing 3% normal horse serum; see Table 1), followed by consecutive incubations with biotinylated secondary antibody (Vector, Burlingame, CA) and streptavidin–peroxidase conjugate (Pierce, Rockford, IL). Color development was achieved using NovaRed substrate kit (Vector) for 3 min. Sections were counterstained with hematoxylin, dehydrated, cleared in histolene, and mounted

in DPX. For fluorescent immunohistochemistry, the method was identical except that streptavidin-conjugated AlexaFluor 594 was used instead of streptavidin–peroxidase conjugate and sections were mounted using anti-fade mounting medium (ProLong Gold, Invitrogen). Specificity of antibody staining was confirmed by incubating adjacent sections with isotype controls (mouse IgG1 and IgG2a isotype controls, 50878 and 553454, BD Pharmingen, San Diego, CA) for monoclonal antibodies or normal rabbit/goat serum for polyclonal rabbit/goat antibodies. For a number of antigens (Brn-3, αB-crystallin, glial fibrillary acidic protein [GFAP], interleukin [IL]-1β, tumor necrosis factor [TNF]-α, PGP 9.5, nestin, tyrosine hydroxylase), a second primary antibody to the same target was used to validate that the labeling pattern obtained was representative. In addition, Western blotting was performed for the majority of antibodies to confirm specificity, in terms of both expected molecular weight and presence within retinal samples.

Immunohistochemical staining was evaluated at the light microscopic level. For each antibody tested, results from Davidson's-fixed sections were compared with those achieved in formalin-fixed sections. Specificity of staining was judged by the morphology and distribution of the labeled cells, by the absence of signal when the primary antibody was replaced by isotype/serum controls, and by comparison with the expected staining pattern based on our own, and other, previously published results. In addition, for some of the less well-documented antibodies, more than one antibody targeted to the antigen was used to validate that the labeling pattern produced was reliable. In these situations, the two antibodies were compared in formalin-fixed tissue. Whichever antibody yielded the best signal-to-noise was then used for the comparison of formalin and Davidson's tissue. The other antibody was not tested, even though it typically provided satisfactory results in formalin tissue. For each antibody tested, a basic, semiquantitative grading scheme was used to evaluate the immunostaining: – = minimal specific labeling; + = weak, specific labeling; ++ = intense, specific labeling.

Antibodies that produced satisfactory labeling in formalin-fixed tissue but were not tested in Davidson's tissue are as follows: mouse anti-αB-crystallin (SPA-222, Stressgen); rabbit anti-IL-1β (ab9787, Abcam); rabbit anti-TNF-α (HP8001, Hycult Uden, The Netherlands); mouse anti-tyrosine hydroxylase (MAB318, Millipore); mouse anti-nestin (clone 25/NESTIN, BD Transduction); and rabbit anti-PGP 9.5 (CL95101, Cedarlane).

### *Western Blotting*

Retinas from uninjured and injured eyes were processed for Western blotting as previously described. (Chidlow et al. 2010). In brief, after electrophoresis, samples were transferred onto polyvinylidene difluoride membranes. Following a block of non-specific binding, blots were probed with primary antibodies, appropriate secondary antibodies conjugated to biotin, and streptavidin–peroxidase conjugate. Blots were then developed and the images captured.

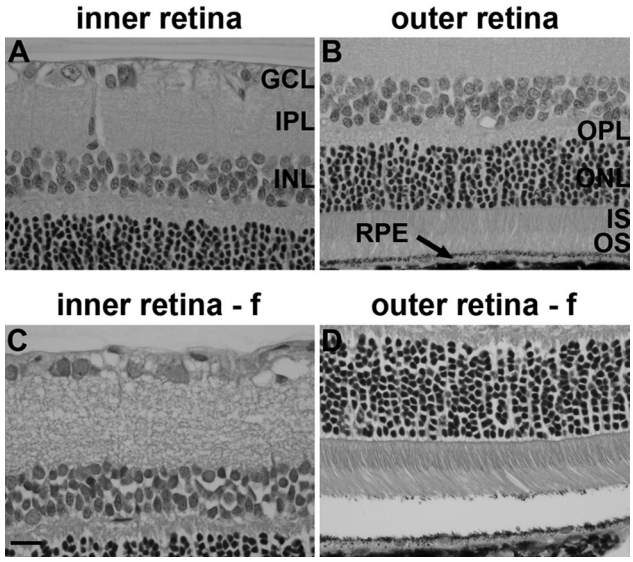


**Figure 1.** Representative images of retinal histology after Davidson's (A, B) and formalin (f; C, D) fixation, as delineated by hematoxylin and eosin staining. Scale bar = 15 µm. GCL, ganglion cell layer; IPL, inner plexiform layer; INL, inner nuclear layer; OPL, outer plexiform layer; ONL, outer nuclear layer; IS, inner segments of photoreceptors; OS, outer segments of photoreceptors; RPE, retinal pigment epithelium.

## Results

### *Histology*

Retinas fixed in Davidson's solution displayed excellent morphological integrity with no detachment of the retina from the RPE (Fig. 1A, B). The morphology of retinas fixed in formalin was satisfactory but inferior to those fixed in Davidson's reagent, featuring less compact and detailed nuclear and plexiform layers (Fig. 1C, D), together with some degree of retinal detachment (Fig. 1D). However, Davidson's-fixed eyes were less straightforward to section than formalin-fixed eyes owing to their brittle nature, a consequence of the alcohol content of Davidson's solution. This was often manifest as lenticular shattering. In addition, slide adherence of sections was less satisfactory in Davidson's-fixed eyes, which was inconsequential regarding hematoxylin and eosin but adversely affected immunohistochemistry.

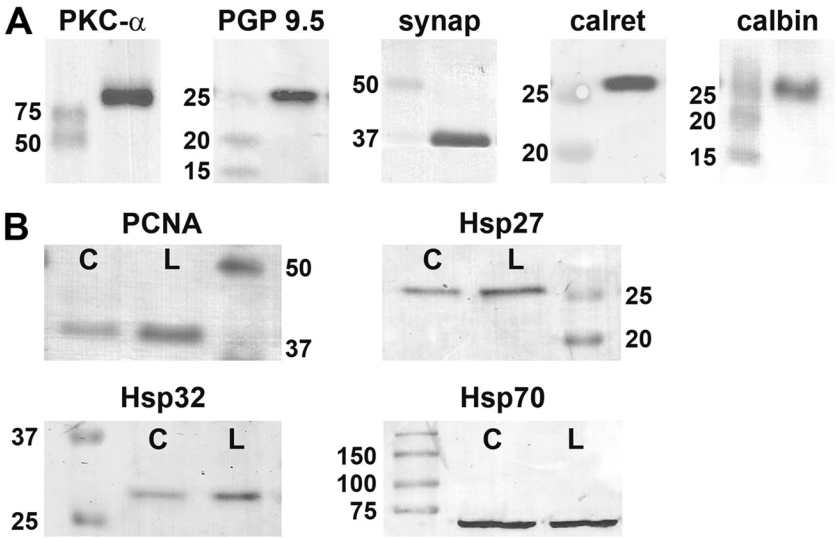


**Figure 2.** Representative images of Western blots of rat retinal samples using various antibodies used in the current study. (A) Expression of protein kinase C (PKC)-α, protein gene product (PGP) 9.5, synaptophysin, calretinin, and calbindin in normal rat retinal samples. (B) Expression of proliferating cell nuclear antigen (PCNA), heat shock protein (Hsp) 27, Hsp32, and Hsp70 in rat retinal samples from control (labeled as C) retinas and from retinas which were lasered 3 days previously (labeled as L).

### *Western Blotting*

To provide additional proof of antibody specificity, Western blotting was performed for many of the antibodies used in the current study. Retinas from control rats or, in the case of inducible proteins, from rats that had received laser treatment 3 days previously were analyzed. Results from 9 of the antibodies tested are shown in Fig. 2. For each of the samples analyzed, a band was visible at the expected molecular weight. For certain proteins induced by injury, for example, Hsp27, Hsp32, and PCNA, a more intense band was observed in the lasered retina compared with the retina from the contralateral eye.

### *Optimization of Immunohistochemistry*

It is well known that the majority of antigens display reduced immunoreactivity after formalin fixation, a phenomenon known as masking. Our previous studies have shown that high-temperature antigen retrieval of formalin-fixed, paraffin-embedded rat ocular sections, comprising microwave heating in citrate buffer pH 6.0 for 10 min at 95–100C, provides an excellent signal-to-background ratio for numerous antigens (Chidlow et al. 2008; Chidlow et al. 2010; Ebneter et al. 2010; Holman et al. 2010; Chidlow et al. 2011). Of the 38 antibodies included in the current study, the citrate retrieval method (in combination with trypsin for two extracellular matrix proteins) in formalin-fixed eyes yielded highly satisfactory results, with intense, specific labeling observed for 37 of the antibodies (Table 2). As would be expected, some antibodies tested during the course of this study, notably those to certain proinflammatory mediators, failed to provide specific staining in our hands. The results from these antibodies (rabbit anti-inducible nitric oxide synthase [iNOS], Sigma, N-7782; rabbit anti-iNOS, Millipore, AB5382; rabbit anti-IL-1β, Santa-Cruz, sc-7884; rabbit anti-IL-6, Abcam, ab6672) are not included.

The optimal conditions for performing immunohistochemistry on Davidson's-fixed tissue are unknown, because there are few published studies that have used the fixative. We tested 8 antibodies (vimentin, calretinin, rhodopsin, synaptophysin, $\beta_3$-tubulin, GFAP, FGF-2, and Hsp32), targeted to a variety of cellular elements, with 3 different high-temperature antigen retrieval methods (citrate pH 6.0, Tris-HCl pH 9.0, EDTA pH 8.0), and one enzyme digestion method (proteinase K), to determine which method produced comparable signal intensities to those detected in formalin-fixed eyes. The use of citrate buffer resulted in weak signals for seven of the eight antibodies tested, vimentin being the robust exception (data not shown). This is unsurprising as the concentration of formaldehyde in Davidson's solution is twice that of formalin, necessitating more vigorous retrieval. Tris-HCl buffer produced stronger labeling than citrate buffer for all nine antibodies but weaker staining than in formalin-fixed tissue (data not shown). EDTA buffer produced robust, specific labeling of intensity comparable to that observed with citrate buffer-retrieved, formalin-fixed sections (Table 2). Proteinase K was totally unsatisfactory as a means of effecting antigen retrieval, eliciting uniformly weak staining patterns (data not shown). As a result of the optimization

**Table 2.** Summary of Compatibility of Each Antibody with Formalin- and Davidson's-Fixed Retinas

| Target | Labeling Intensity | | Target | Labeling Intensity | |
|---|---|---|---|---|---|
| | Formalin | Davidson | | Formalin | Davidson |
| Brn-3 | ++ | + | Interleukin-1β | ++ | ++ |
| Brn3a | ++ | ++ | Interleukin-6 | ++ | ++ |
| Calbindin | ++ | ++ | Inducible nitric oxide synthase | ++ | + |
| Calretinin | ++ | ++ | Laminin | ++ | ++ |
| CD3 | ++ | ++ | Monocarboxylate transporter-3 | ++ | ++ |
| Choline acetyl transferase | ++ | ++ | Major histocompatibility complex II | ++ | ++ |
| Chx10 | ++ | ++ | Myeloperoxidase | ++ | ++ |
| Cyclooxygenase-2 | ++ | ++ | Nestin | ++ | + |
| Ciliary neurotrophic factor | ++ | ++ | Parvalbumin | ++ | ++ |
| αB-crystallin | ++ | + | Proliferating cell nuclear antigen | ++ | ++ |
| ED1 | ++ | ++ | Protein gene product 9.5 | ++ | ++ |
| Collagen VI | ++ | ++ | Protein kinase C-α | ++ | ++ |
| Fibroblast growth factor-2 | ++ | ++ | RPE-65 | ++ | ++ |
| γ-Aminobutyric acid | ++ | — | Rhodopsin (RET-P1) | ++ | ++ |
| Glial fibrillary acidic protein | ++ | ++ | Synaptophysin | ++ | ++ |
| Glutamine synthetase | ++ | ++ | Tumor necrosis factor -α | ++ | ++ |
| Heat shock protein-27 | ++ | + | $\beta_3$-tubulin | ++ | ++ |
| Heat shock protein-32 | ++ | ++ | Tyrosine hydroxylase | ++ | ++ |
| Heat shock protein-70 | + | + | Vimentin | ++ | ++ |
| Iba1 | ++ | + | | | |

Grading scheme: – = minimal specific labeling, + = weak, specific labeling, ++ = intense, specific labeling.

experiments, EDTA buffer was routinely used for antigen retrieval for all 38 antibodies tested in this study. All of the images presented in the Results figures show sections from Davidson's-fixed retinas, unless otherwise stated in the plate and accompanying legend.

## *Neuronal Markers*

The retina comprises four major classes of neurons: retinal ganglion cells (RGCs) (the output neurons of the retina whose axons form the optic nerve), amacrine cells, bipolar cells, and horizontal cells, each of which can be further subdivided into subclasses. The retina also contains a specialized class of neurons, the light-sensitive photoreceptors. There is, to our knowledge, no recognized pan-neuronal marker of retinal neurons. The classical central nervous system pan-neuronal marker, protein gene product (PGP) 9.5, was robustly expressed by RGCs, amacrine cell, and horizontal cell somata and their processes, but not by bipolar cells, in our formalin- and Davidson's-fixed retinas (Fig. 3A). Delineation of horizontal cells is straightforward because of their discrete location, but the presence of a substantial number of amacrine cells in the ganglion cell layer (GCL) of the rat means that PGP 9.5 cannot be used to selectively identify RGCs. A number of RGC-specific markers have been developed over the years. We tested two commonly used antibodies directed against the microtubule element $\beta_3$-tubulin and the transcription factor Brn-3. $\beta_3$-Tubulin immunoreactivity (Fig. 3B) was associated with RGC somata, axons, and the finely detailed meshwork of dendrites in the inner plexiform layer (IPL), whereas Brn-3 was localized to RGC nuclei (Fig. 3C). Identical patterns of staining were displayed with both fixatives, but Brn-3 labeling was weaker in Davidson's-fixed tissue. The definitive marker of bipolar cells, clone MC5, which recognizes protein kinase C (PKC)-α, yielded excellent staining with both fixatives, precisely demarcating cell bodies as well as the pre- and postsynaptic terminals with photoreceptors and RGCs, respectively (Fig. 3D), whereas an alternative marker of bipolar cells, Chx10, was associated with cell nuclei (data not shown). The widely used clone RET-P1, which targets rhodopsin, reliably labeled photoreceptors in formalin and Davidson's sections (Fig. 3E). Calretinin, parvalbumin, and calbindin are members of a family of low-molecular-weight calcium-binding proteins expressed in specific neuron populations of the retina. Antibodies directed against all three proteins produced strong, specific labeling patterns in formalin- and Davidson's-fixed tissue. Calretinin immunoreactivities were found in somata in the inner nuclear layer (INL) and GCL together with the characteristic three strata of terminals in the IPL (Fig. 3F). Parvalbumin immunoreactivities

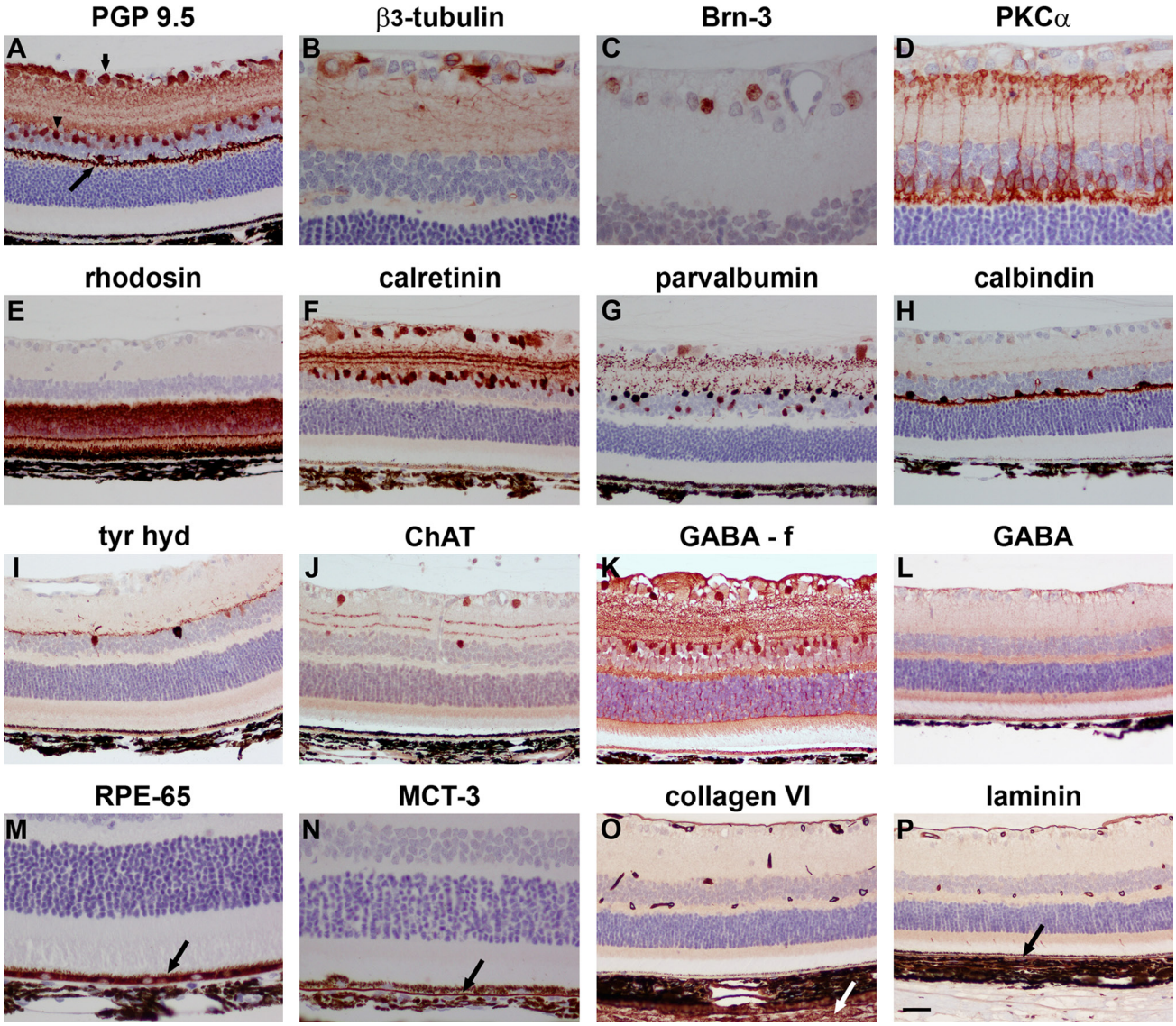


**Figure 3.** Representative images of neuronal and non-neuronal markers in Davidson's- and formalin- (f) fixed retinas, as shown by immunohistochemistry. (A) Retinal ganglion cells (RGCs) (short arrow), amacrine cells (arrowhead), and horizontal cells (long arrow) labeled by the pan-neuronal marker PGP 9.5. (B) RGC somata, dendrites, and axons labeled by $\beta_3$-tubulin. (C) RGC nuclei labeled by Brn-3. (D) Bipolar cells and their processes terminating in the inner and outer plexiform layers labeled by protein kinase C (PKC)-α. (E) Photoreceptor cell bodies and their segments labeled by rhodopsin. (F) Amacrine cells and RGCs labeled by calretinin with 3 layers of terminals visible in the inner plexiform layer (IPL). (G) RGCs, amacrine cells, and their terminals labeled by parvalbumin. (H) Horizontal cells and their processes labeled by calbindin. (I) Putative dopaminergic amacrine cells as labeled by tyrosine hydroxylase (tyr hyd). (J) Putative cholinergic amacrine cells and 2 layers of terminals visible in the IPL as labeled by choline acetyl transferase (ChAT). (K) GABAergic amacrine cells as labeled by GABA in a formalin-fixed retina. (L) Lack of GABA immunolabeling in a Davidson's-fixed retina. (M) Retinal pigment epithelium (RPE) labeled by RPE-65. (N) Basolateral surface of RPE labeled by MCT3. (O) Labeling of inner limiting membrane, blood vessels, and sclera (arrow) by collagen VI. (P) Labeling of inner and outer (arrow) limiting membrane and blood vessels by laminin. Scale bar: B-D, M, N = 15 µm; A, E-L, O, P = 30 µm.

were found in AII-type amacrine cells, some RGCs, and punctate AII terminals in the IPL (Fig. 3G). Calbindin immunoreactivity was predominantly associated with horizontal cell somata and their dendrites in the outer plexiform layer (OPL; Fig. 3H).

Further neuronal markers of interest are those that identify neurotransmitter-synthesizing cells. Dopaminergic and cholinergic neurons in the retina can be identified by labeling for tyrosine hydroxylase and choline acetyl transferase, respectively, and antibodies directed against these targets clearly

delineated two populations of amacrine cells in both formalin- and Davidson's-fixed tissue (Fig. 3I, J). In contrast, a well-characterized antibody to the major inhibitory neurotransmitter of the retina, γ-aminobutyric acid (GABA), provided satisfactory staining in formalin-fixed retinas (Fig. 3K), but was incompatible with Davidson's solution, yielding only nonspecific staining (Fig. 3L).

### *Retinal Pigment Epithelial and Extracellular Matrix Markers*

Retinal pigment epithelium (RPE) cells were labeled using two well-established markers, RPE-65 and monocarboxylate transporter-3 (MCT-3), which are exclusively expressed by this monolayer of cells. RPE-65, which plays a role in phototransduction, was observed throughout the cytoplasm of RPE cells (Fig. 3M), whereas MCT-3 was discretely localized to the basal membrane (Fig. 3N). Similar results were achieved in formalin- and Davidson's-fixed tissue.

Antibodies directed against the extracellular matrix proteins collagen VI and laminin specifically labeled blood vessels and the inner limiting membrane in formalin- and Davidson's-fixed sections (Fig. 3O, P). In addition, collagen VI stained the sclera, whereas laminin labeled Bruch's membrane.

### *Macroglia*

Two types of macroglia reside within the retina: Müller cells and astrocytes. Müller cells, the principal glial cells of the retina, are radial glia, whose processes span the thickness of the retina. Astrocytes, which enter the retina along the developing optic nerve, are flattened cells restricted to the vitreal surface of the retina. In normal retinas, antibodies directed against the intermediate filament vimentin (Fig. 4A) and the glutamate-metabolizing enzyme glutamine synthetase (Fig. 4B) labeled both astrocytes and Müller cells, with the former restricted to processes, whereas the latter also identified somata. After treatment with LPS or argon laser, hypertrophy of both cell types was evident from the vimentin and glutamine synthetase staining patterns (data not shown). Another intermediate filament, GFAP, was expressed by astrocytes but was largely absent from Müller cells in normal retinas (Fig. 4C). Following LPS or argon laser injury, a robust upregulation of GFAP was detected in Müller cell processes (Fig. 4D). For vimentin, glutamine synthetase, and GFAP, similar intensity and signal-to-background patterns of staining were observed in formalin- and Davidson's-fixed tissue.

Following injury to the retina, Müller glia undergo dedifferentiation, which can be detected by labeling for a third intermediate filament, nestin, a commonly used marker of neural progenitor cells. In normal, formalin-fixed retinas, nestin immunoreactivity was restricted to blood vessels (data not shown). By 6 hr after LPS injury, limited upregulation of nestin immunoreactivity was detected in astrocytes and Müller cell processes (Fig. 4E). At 24 hr after laser injury, a dramatic upregulation of nestin was observed (Fig. 4G). Compared with formalin-fixed retinas, nestin immunoreactivities in Davidson's-fixed retinas were considerably less abundant (Fig. 4F, H).

### *Microglia, Infiltrating White Cells*

Microglia are exquisitely sensitive to any disruption of neuronal homeostasis, responding in a well-defined manner. As such, they serve as valuable indicators of neurotoxicity. The traditional marker of resting and activated microglia, clone OX-42, which identifies the rat equivalent of complement type 3 receptor cd11b, is incompatible with formalin-fixed paraffin-embedded sections and likewise produced no positive staining in Davidson's-fixed sections (data not shown). An alternative, increasingly used marker of resting and activated microglia is iba1. In formalin-fixed sections, iba1-labeling was strong and defined (Fig. 4I). In Davidson's-fixed sections, iba1 staining at the same dilution of antibody was weak (Fig. 3J). Even 10-fold more concentrated, iba1 labeling was poor compared with formalin, with processes in particular ill-defined (Fig. 4K).

ED1 and OX-6, which recognize the rat equivalents of human CD68 and MHC class II, were absent from normal retinas. In laser-damaged retinas, ED1-positive and OX-6–positive microglia (Fig. 4L, M) and infiltrating ED1-positive macrophages (data not shown) were readily identified, displaying similar profiles in formalin- and Davidson's-fixed sections. Detection of infiltrating neutrophils and the occasional T cell after laser damage was successfully achieved using antibodies against myeloperoxidase and CD3, respectively (Fig. 4N, O). Again, similar results were obtained with formalin- and Davidson's-fixed tissue.

### *Proinflammatory Mediators and Cell Proliferation*

No expression of any of the proinflammatory cytokines IL-1β, TNF-α, IL-6, cyclooxygenase-2 (COX-2), or iNOS was detected in normal formalin- or Davidson's-fixed tissue sections (data not shown). Intravitreal administration of the classical proinflammatory toxin LPS induced a rapid upregulation of all five molecules. IL-1β, TNF-α, and IL-6 were all localized to subsets of microglia in the inner retina. The involvement of microglia was confirmed by double labeling with iba1 (data not shown). IL-1β was expressed by the majority of microglia (Fig. 5A); TNF-α was observed in substantially fewer cells, which were often of amoeboid morphology (Fig. 5B); IL-6 was expressed in fewer cells again (Fig. 5C). iNOS immunoreactivity was rarely observed in the retina but was observed in many cells

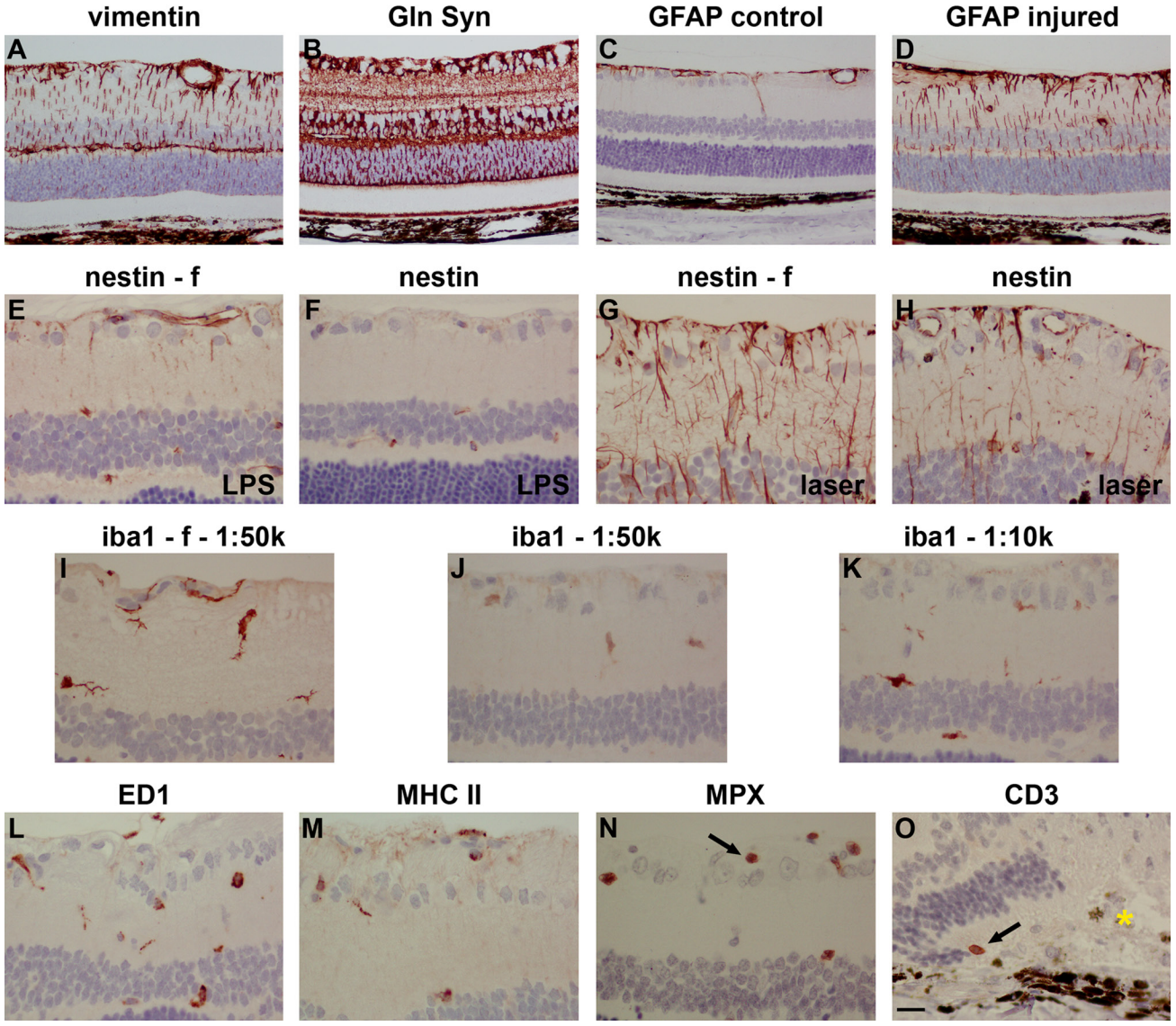


**Figure 4.** Representative images of macroglia (astrocytes and Müller cells), microglia, neutrophils, and T cells in Davidson's- and formalin-(f) fixed retinas, as shown by immunohistochemistry. Müller cell and astrocytes in a normal retina labeled by (A) vimentin and (B) glutamine synthetase (Gln Syn). Glial fibrillary acidic protein (GFAP) labeling of astrocytes in a normal retina (C). Upregulated GFAP expression in astrocytes and Müller cell processes following laser photocoagulation (D). Nestin labeling in Davidson's- and formalin-fixed retinas after lipopolysaccharide (LPS) treatment (E, F) and laser photocoagulation (G, H). In both cases, nestin immunoreactivity was weaker in Davidson's-fixed retinas compared with those fixed in formalin. (I) Microglia in a normal, formalin-fixed retina labeled by iba1. (J, K) In normal, Davidson's-fixed retinas, iba1 labeling was weaker, even at 5-fold higher concentration of antibody. (L) Phagocytic microglia labeled by ED1 following laser photocoagulation. (M) Major histocompatibility complex (MHC) class II–positive microglia following laser photocoagulation. (N) Neutrophils labeled by myeloperoxidase (MPX) following laser photocoagulation. (O) A T cell labeled by CD3 following laser photocoagulation. The gold asterisk indicates the position of the laser lesion. Scale bar: A-D = 30 µm; E-O = 15 µm.

at the limbus (Fig. 5D), whereas COX-2 immunoreactivity was exclusively localized to endothelial cells in the GCL (Fig. 5E). For each of these markers, with the exception of iNOS, which was somewhat weaker in Davidson's, similar intensity and signal-to-background patterns of staining were observed in formalin- and Davidson's-fixed tissue.

To identify cell proliferation, we labeled tissue sections from laser-damaged retinas with an antibody against

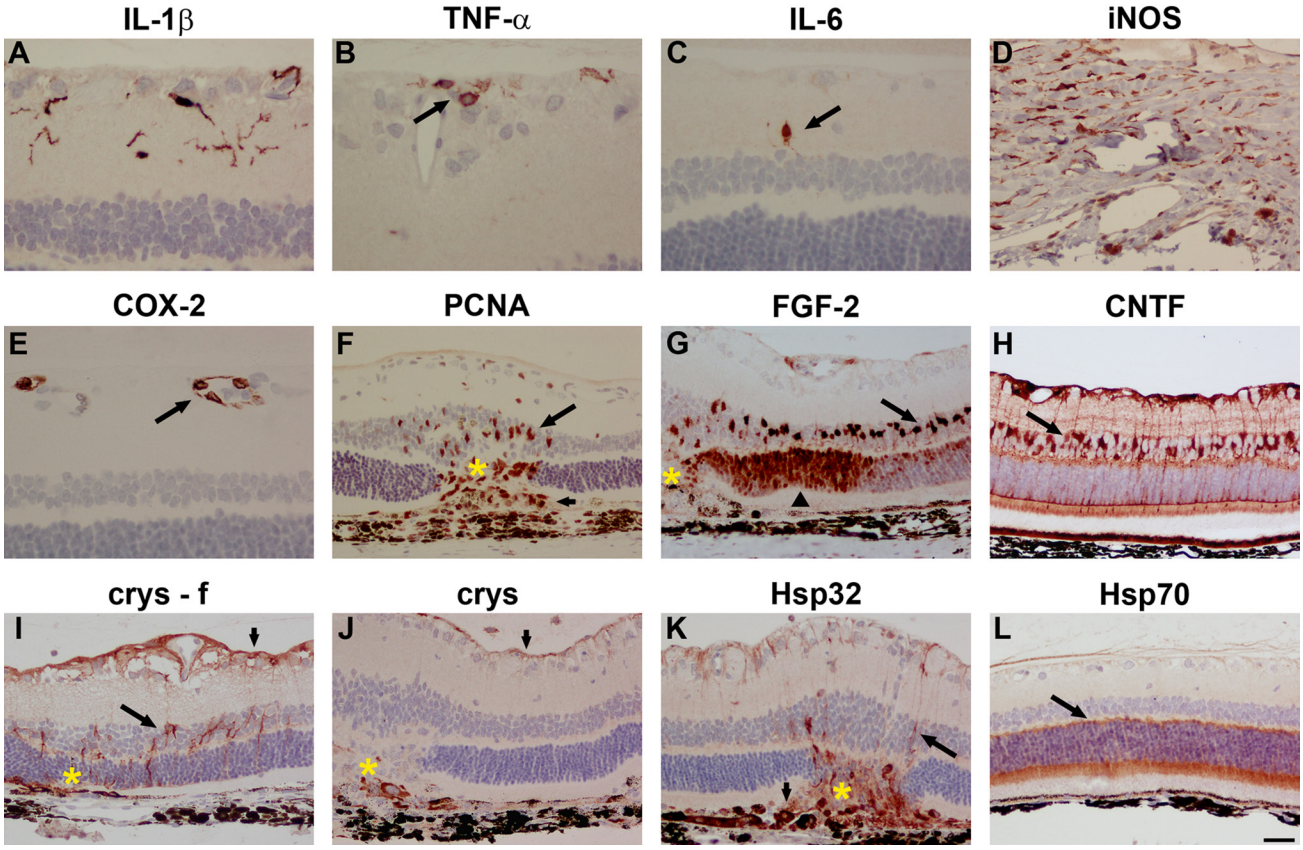


**Figure 5.** Representative images of trauma-induced proinflammatory mediators, cell proliferation, trophic factors, and heat shock proteins (Hsps) in Davidson's- and formalin- (f) fixed retinas, as shown by immunohistochemistry. Interleukin (IL)-1β (A), tumor necrosis factor (TNF)-α (B, arrow), and IL-6 (C, arrow) expression by microglia following lipopolysaccharide (LPS) treatment. (D) Inducible nitric oxide synthase (iNOS) expression in limbal cells following LPS treatment. (E) Cyclooxygenase-2 (COX-2) expression in endothelial cells (arrow) following LPS treatment. (F) Upregulation of proliferating cell nuclear antigen (PCNA) in Müller cells (long arrow) and infiltrating cells (short arrow) following laser photocoagulation. (G) Upregulated fibroblast growth factor-2 (FGF-2) expression in Müller cells (long arrow) and photoreceptors (arrowhead) following laser photocoagulation. (H) Upregulated ciliary neurotrophic factor (CNTF) expression in Müller cells (long arrow) and astrocytes (short arrow) following laser photocoagulation. In formalin-fixed tissue (I), αB-crystallin expression is associated with astrocytes (short arrow) and Müller cells (long arrow) following laser photocoagulation, but in Davidson's-fixed tissue (J), laser photocoagulation-induced αB-crystallin expression is markedly weaker. (K) Hsp32 expression associated with Müller cell processes (arrow) and infiltrating macrophages (short arrow) following laser photocoagulation. (L) Hsp70-positive photoreceptors (arrow) in a normal retina. Gold asterisks indicate laser lesions. Scale bar: A-C, E = 15 μm; D, F-L = 30 μm.

proliferating cell nuclear antigen (PCNA). Müller cell nuclei overlying the lesion, but not elsewhere, were PCNA-positive, together with the nuclei of infiltrating cells (Fig. 5F), whereas PCNA produced satisfactory staining in formalin- and Davidson's-fixed tissue.

## *Trophic Factors*

In normal retinas, fibroblast growth factor-2 (FGF-2) expression was restricted to Müller cell somata (data not shown). Following laser damage, FGF-2 was upregulated in Müller cells and synthesized de novo by photoreceptors, particularly adjacent to the lesion site (Fig. 5G). In normal retinas, ciliary neurotrophic factor (CNTF) was expressed by astrocytes, Müller cell somata, and some Müller process spanning the retina (data not shown). Following laser damage, CNTF expression by both astrocytes and Müller cells increased (Fig. 5H). Similar intensity and signal-to-background patterns of staining were observed in formalin- and Davidson's-fixed tissue.

## *Heat Shock Proteins (Hsps)*

Hsps are an important group of cellular stress response proteins that are induced by a myriad of stimuli. In normal retinas, astrocytes in the nerve fiber layer expressed low

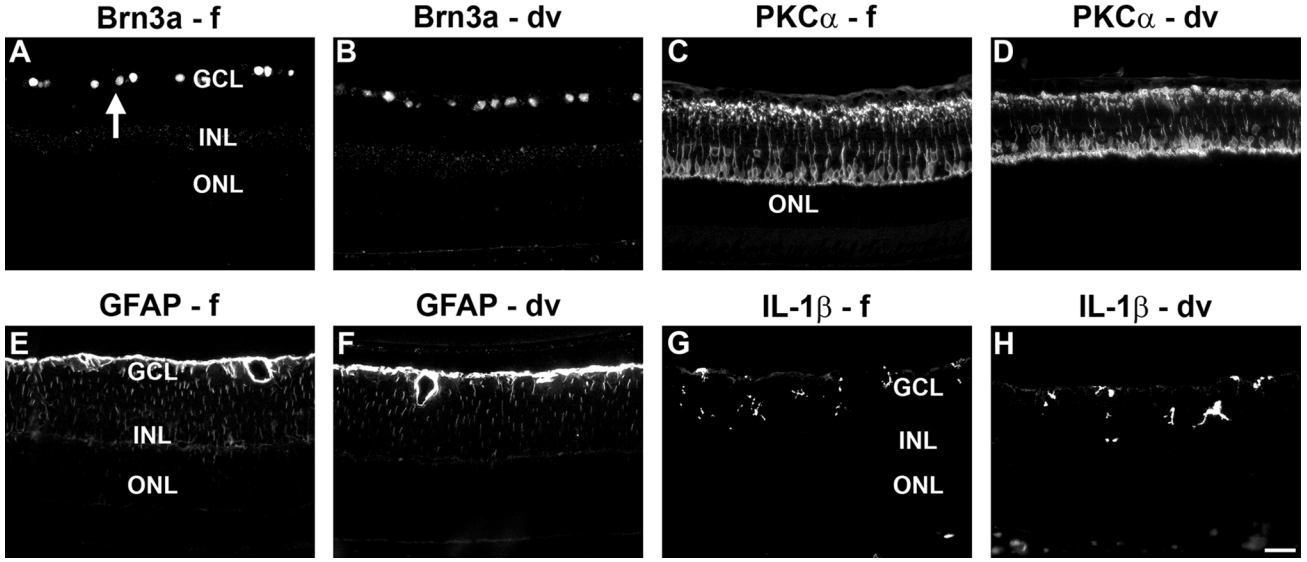


**Figure 6.** Representative images of neuronal and non-neuronal markers in formalin-fixed (f) and Davidson's-fixed (dv) retinas, as shown by fluorescent immunohistochemistry. Retinal ganglion cell (RGC) nuclei (arrow) labeled by Brn-3a (A, B) and bipolar cells and their processes labeled by protein kinase C (PKC)-α (C, D) in normal retinas. Astrocytes and Müller cells labeled by glial fibrillary acidic protein (GFAP) (E, F) and microglia labeled by interleukin (IL)-1β (G, H) in retinas of lipopolysaccharide (LPS)-injected eyes. Scale bar = 30 μm. GCL, ganglion cell layer; INL, inner nuclear layer; ONL, outer nuclear layer.

levels of the small Hsps αB-crystallin and Hsp27 (data not shown). Following laser damage, αB-crystallin (Fig. 5I) and Hsp27 (data not shown) were both upregulated by astrocytes and synthesized de novo by Müller cells and RGCs, respectively, in the vicinity of the lesion. Both small Hsps produced weaker labeling in Davidson's-fixed tissue, as shown for αB-crystallin (Fig. 5J). No Hsp32 immunoreactivity was observed in normal retinas (data not shown). Following laser damage, Hsp32-positive macrophages infiltrated the lesion site, and some expression of Hsp32 was associated with Müller cell processes (Fig. 5K). Hsp70 was constitutively expressed by photoreceptors but was largely unchanged after laser photocoagulation (Fig. 5L). Unlike the small Hsps, Hsp32 and Hsp 70 stained equally well in formalin- and Davidson's-fixed tissue.

### *Immunofluorescence*

As a final component to the study, we investigated whether Davidson's-fixed tissue was compatible with fluorescent immunohistochemistry. We tested various antibodies that displayed similar intensity labeling patterns in formalin- and Davidson's-fixed tissue when visualized by immunoperoxidase staining. Sample results from two neuronal markers (Brn3a and PKC-α) and two glial markers (GFAP and IL-1β) are shown in Fig. 6. For each antibody and each fixative, similar results were generated to those obtained by immunoperoxidase staining, indicating the utility of Davidson's fixative with fluorescent immunohistochemistry.

## Discussion

Davidson's solution has long been advocated as the optimal fixative for whole eyes, providing excellent tissue morphology while avoiding retinal detachment (Heywood and Gopinath 1990; Latendresse et al. 2002; Morawietz et al. 2004; McKay et al. 2009). Yet the fixative has only rarely been used in concert with immunohistochemistry (Chidlow et al. 2005; Kercher et al. 2007), and its compatibility has accordingly remained largely unexplored. The potential use of Davidson's-fixed tissue for immunohistochemical purposes is attractive, especially in those studies that would benefit from the excellent morphology and the correct apposition of the photoreceptors with the RPE. These include studies involving rodent models of photoreceptor degeneration; investigations into the effects of insults acting at the level of the retina RPE, for example, by photocoagulator lasers; and neurotoxicological studies.

In the current study, we have validated 39 antibodies in control and experimentally injured retinas in formalin- and Davidson's-fixed, paraffin-embedded sections using immunoperoxidase and fluorescent immunohistochemistry protocols. Each antibody produced a pattern of immunoreactivity consistent with expectations from the published literature. In general, the cellular and subcellular patterns obtained with each fixative were identical; moreover, the abundance of immunoreactivity obtained with each antibody was comparable. Thus, for the majority of antibodies tested, Davidson's solution provided arguably superior results, simply as a result of the better preserved morphology of the

tissue sections and the absence of any artifactual retinal detachment. Our results correspond with the recent findings of McKay et al. (2009), who stained formalin- and Davidson's-fixed normal rat retinas for four cellular markers: rhodopsin, synaptophysin, glutamine synthetase, and GFAP, markers of photoreceptors, neuronal synapses, radial glial cells, and astrocytes, respectively, and concluded that the latter fixative was superior. However, McKay et al. further noted that formalin-fixed sections featured poor cellular detail together with some non-specific staining and were difficult to cut. This was demonstrably not the case in our study, where the morphological preservation of formalin-fixed sections was highly acceptable for interpretation of immunohistochemical staining and appreciably better than could be obtained with cryosections. We can only conclude that the method used to produce formalin-fixed sections in the latter study was suboptimal, given that numerous studies, including many from our own laboratory (Chidlow et al. 2008; Chidlow et al. 2010; Ebneter et al. 2010; Holman et al. 2010; Chidlow et al. 2011), have produced high-quality results from formalin-fixed sections.

The antibodies used in the present study allow unequivocal identification of a wide range of retinal cellular targets in Davidson's-fixed tissue and will prove useful for basic science studies as well as toxicological risk assessment. Retinal neuronal loss can be easily assessed by labeling for PGP 9.5, which robustly demarcates RGCs, amacrine cells, and horizontal cells (Chen et al. 1994), together with PKC-α, the stereotypical marker of bipolar cells, which additionally identifies postsynaptic connections with RGCs in superb definition (Wassle et al. 1991). The calcium-binding proteins calretinin, parvalbumin, and calbindin label a mixture of horizontal cells, amacrine cells, and RGCs and their processes. They are widely used in retinal research as markers after injuries such as ischemia and excitotoxicity (Osborne and Larsen 1996; Yamamoto et al. 2006; Kim et al. 2010). The Brn-3 family of proteins, including the most commonly used member Brn3a, are localized exclusively to RGC nuclei and are routinely used as a tool for quantitative assessment of RGC death in models of experimental glaucoma and optic nerve damage (Weishaupt et al. 2005; Nadal-Nicolas et al. 2009; Salinas-Navarro et al. 2010; Sanchez-Migallon et al. 2011). Additional neuronal biomarkers of interest include antibodies to the major neurotransmitter systems of the retina, which are rapidly affected in situations of neuronal perturbation (Osborne et al. 1995). Retinal macroglia, namely astrocytes and Müller cells, respond rapidly to all types and degrees of neuronal injury in well-defined ways. Vimentin and glutamine synthetase are constitutively expressed by both cell types and are both upregulated in response to injury (Bringmann et al. 2006), whereas GFAP is the most commonly used immunohistochemical marker of homeostatic imbalance in the retina. Upregulated GFAP represents a universal and sensitive response to retinal injury (Bringmann et al. 2006). Similar to macroglia, retinal microglia are exquisitely sensitive to neuronal perturbation (Langmann 2007). Iba1 demarcates both quiescent and activated microglia (Ito et al 1998, 2001), while ED1, which recognizes the rat equivalent of human CD68, provides clear, unambiguous data relating to microglial phagocytosis. Both markers are routinely exploited by retinal researchers. Other markers of interest analyzed in the current study include antibodies directed against inducible Hsps, growth factors, and proinflammatory mediators. In conditions of neuronal and glial stress, these molecules are subject to dynamic regulation, acting as part of the endogenous survival response of the retina. For example, various insults to the rat retina, including intense light (Wen et al. 1998), trauma (Wen et al. 1995), ischemia (Ju et al. 1999), and excitotoxicity (Honjo et al. 2000), all result in an upregulation of the growth factors FGF-2 and CNTF. In the current study, we observed increased macroglial expression of both molecules, and de novo expression of FGF-2 by photoreceptors, after laser-induced injury in both formalin- and Davidson's-fixed tissue. To monitor inflammation, we characterized various antibodies directed against proinflammatory mediators. These can be difficult to localize immunohistochemically, owing to their rapid synthesis and release combined with a lack of compatibility of some antibodies in paraffin sections; however, we achieved high signal-to-background labeling in Davidson's- as well as formalin-fixed tissue.

Despite the advantages of Davidson's-fixed sections, two issues temper enthusiasm over the use of the method. The first issue concerns retention of sections on slides. High-temperature antigen retrieval using EDTA frequently resulted in partial detachment of the tissue section from the slide. This occurred despite the use of highly adherent slides (SuperFrost Ultra Plus), which are specifically designed for sections that undergo microwave-assisted, heat-induced antigen retrieval. The retinal tissue itself was unaffected, but the harder, collagen-rich sclera, cornea, and lens were often twisted and found overlying the retina. An explanation can be found in the alcohol content of Davidson's, which causes sections to be more brittle than those fixed in formalin, together with the higher pH of EDTA compared with citrate, which contributes to its stronger retrieval action but can result in detachment (Shi et al. 1995; Pileri et al. 1997).

The second, and more concerning, issue with the use of Davidson's fixative is related to its relative incompatibility with certain antibodies. This was most strikingly illustrated by immunostaining for the neurotransmitter GABA, which yielded no specific signal in Davidson's-fixed tissue. It was equally relevant for the markers iba1 (Bosco et al. 2008; Holman et al. 2010; Oharazawa et al. 2010), nestin (Xue et al. 2006; Chang et al. 2007), and the small Hsps αB-crystallin and Hsp27 (Li et al. 2003; Kalesnykas et al. 2007;

Kalesnykas et al. 2008; Schmeer et al. 2008), all of which are important biomarkers of retinal stress in experimental studies and prime candidates for use in a panel of antibodies selected for toxicological risk assessment. The iba1 results are of particular concern, because the most suitable alternative marker of both quiescent and activated microglia, OX-42, is non-reactive in paraffin tissue. For iba1, nestin, αB-crystallin, and Hsp27, weaker labeling was evident in Davidson's-fixed retinas compared with sections fixed in formalin, which could not be resolved satisfactorily by increasing the concentration of the primary antibody or by combining high temperature and enzyme retrieval techniques. The risk is that increased expression of these biomarkers, manifest as elevated immunoreactivities compared with vehicle-treated samples, would be underestimated if Davidson's fixative was used. There are possibilities by which an enhanced signal could be attained. One approach would be to alter the formulation of Davidson's solution such that it contains a lower concentration of the dehydrating agent, ethanol. This tactic has been shown to be successful with Davidson's solution in the rat testes (Latendresse et al. 2002), but the altered formulation when used to fix rat eyes elicited partial retinal detachment, to some extent defeating the purpose of using the fixative. An alternative approach would be to use a higher pH antigen retrieval solution, such as Tris-HCl pH 10.0 (Shi et al. 1995; Evers and Uylings 1997; Pileri et al. 1997), but this would cause even greater problems with tissue adherence. A third alternative would be to use detection phase amplification, for example, tyramine signal amplification (von Wasielewski et al. 1997). The drawback is that this technique can be highly variable (Mengel et al. 1999). The overall results of this study support the use of Davidson's solution for immunohistochemistry of the rat retina, but with the caveat that it may not be suitable for analysis of every antigen that can be used in conjunction with formalin.

## Acknowledgment

The authors are grateful to Malcolm Plunkett of Ellex R&D Pty Ltd for expert technical assistance with the photocoagulator laser and to Jim Manavis of SA Pathology for helpful discussions.

## Declaration of Conflicting Interests

The author(s) declared no potential conflicts of interest with respect to the authorship and publication of this article.

## Funding

The author(s) disclosed receipt of the following financial support for the research, authorship, and/or publication of this article: Research supported in part by Ellex R&D Pty Ltd.

## References

Bosco A, Inman DM, Steele MR, Wu G, Soto I, Marsh-Armstrong N, Hubbard WC, Calkins DJ, Horner PJ, Vetter ML. 2008. Reduced retina microglial activation and improved optic nerve integrity with minocycline treatment in the DBA/2J mouse model of glaucoma. Invest Ophthalmol Vis Sci. 49:1437–1446.

Bringmann A, Pannicke T, Grosche J, Francke M, Wiedemann P, Skatchkov SN, Osborne NN, Reichenbach A. 2006. Muller cells in the healthy and diseased retina. Prog Retin Eye Res. 25:397–424.

Chang ML, Wu CH, Jiang-Shieh YF, Shieh JY, Wen CY. 2007. Reactive changes of retinal astrocytes and Muller glial cells in kainate-induced neuroexcitotoxicity. J Anat. 210:54–65.

Chen ST, von Bussmann KA, Garey LJ, Jen LS. 1994. Protein gene product 9.5-immunoreactive retinal neurons in normal developing rats and rats with optic nerve or tract lesion. Brain Res Dev Brain Res. 78:265–272.

Chidlow G, Ebneter A, Wood JP, Casson RJ. 2011. The optic nerve head is the site of axonal transport disruption, axonal cytoskeleton damage and putative axonal regeneration failure in a rat model of glaucoma. Acta Neuropathol. 121:737–51.

Chidlow G, Holman MC, Wood JP, Casson RJ. 2010. Spatiotemporal characterization of optic nerve degeneration after chronic hypoperfusion in the rat. Invest Ophthalmol Vis Sci. 51:1483–1497.

Chidlow G, Wood JP, Graham M, Osborne NN. 2005. Expression of monocarboxylate transporters in rat ocular tissues. Am J Physiol Cell Physiol. 288:C416–C428.

Chidlow G, Wood JP, Manavis J, Osborne NN, Casson RJ. 2008. Expression of osteopontin in the rat retina: effects of excitotoxic and ischemic injuries. Invest Ophthalmol Vis Sci. 49:762–771.

Ebneter A, Casson RJ, Wood JP, Chidlow G. 2010. Microglial activation in the visual pathway in experimental glaucoma: spatiotemporal characterisation and correlation with axonal injury. Invest Ophthalmol Vis Sci. 51:6448–6460.

Evers P, Uylings HB. 1997. An optimal antigen retrieval method suitable for different antibodies on human brain tissue stored for several years in formaldehyde fixative. J Neurosci Meth. 72:197–207.

Fritschy JM. 2008. Is my antibody-staining specific? How to deal with pitfalls of immunohistochemistry. Eur J Neurosci. 28:2365–2370.

Heywood R, Gopinath C. 1990. Morphological assessment of visual dysfunction. Toxicol Pathol. 18:204–217.

Holman MC, Chidlow G, Wood JP, Casson RJ. 2010. The effect of hyperglycemia on hypoperfusion-induced injury. Invest Ophthalmol Vis Sci. 51:2197–2207.

Honjo M, Tanihara H, Kido N, Inatani M, Okazaki K, Honda Y. 2000. Expression of ciliary neurotrophic factor activated by retinal Muller cells in eyes with NMDA- and kainic acid-induced neuronal death. Invest Ophthalmol Vis Sci. 41:552–560.

Ito D, Imai Y, Ohsawa K, Nakajima K, Fukuuchi Y, Kohsaka S. 1998. Microglia-specific localisation of a novel calcium binding protein, Iba1. Brain Res Mol Brain Res. 57:1–9.

Ito D, Tanaka K, Suzuki S, Dembo T, Fukuuchi Y. 2001. Enhanced expression of Iba1, ionized calcium-binding adapter molecule

1, after transient focal cerebral ischemia in rat brain. Stroke. 32:1208–1215.

Ju WK, Lee MY, Hofmann HD, Kirsch M, Chun MH. 1999. Expression of CNTF in Muller cells of the rat retina after pressure-induced ischemia. Neuroreport. 10:419–422.

Kalesnykas G, Niittykoski M, Rantala J, Miettinen R, Salminen A, Kaarniranta K, Uusitalo H. 2007. The expression of heat shock protein 27 in retinal ganglion and glial cells in a rat glaucoma model. Neuroscience. 150:692–704.

Kalesnykas G, Tuulos T, Uusitalo H, Jolkkonen J. 2008. Neurodegeneration and cellular stress in the retina and optic nerve in rat cerebral ischemia and hypoperfusion models. Neuroscience. 155:937–947.

Kercher L, Favara C, Striebel JF, LaCasse R, Chesebro B. 2007. Prion protein expression differences in microglia and astroglia influence scrapie-induced neurodegeneration in the retina and brain of transgenic mice. J Virol. 81:10340–10351.

Kim SA, Jeon JH, Son MJ, Cha J, Chun MH, Kim IB. 2010. Changes in transcript and protein levels of calbindin D28k, calretinin and parvalbumin, and numbers of neuronal populations expressing these proteins in an ischemia model of rat retina. Anat Cell Biol. 43:218–229.

Langmann T. 2007. Microglia activation in retinal degeneration. J Leukoc Biol. 81:1345–1351.

Latendresse JR, Warbrittion AR, Jonassen H, Creasy DM. 2002. Fixation of testes and eyes using a modified Davidson's fluid: comparison with Bouin's fluid and conventional Davidson's fluid. Toxicol Pathol. 30:524–533.

Li Y, Roth S, Laser M, Ma JX, Crosson CE. 2003. Retinal preconditioning and the induction of heat-shock protein 27. Invest Ophthalmol Vis Sci. 44:1299–1304.

McKay JS, Steele SJ, Ahmed G, Johnson E, Ratcliffe K. 2009. An antibody panel for immunohistochemical analysis of the retina in Davidson's-fixed, paraffin-embedded eyes of rats. Exp Toxicol Pathol. 61:91–100.

Mengel M, Werner M, von Wasielewski R. 1999. Concentration dependent and adverse effects in immunohistochemistry using the tyramine amplification technique. Histochem J. 31:195–200.

Morawietz G, Ruehl-Fehlert C, Kittel B, Bube A, Keane K, Halm S, Heuser A, Hellmann J. 2004. Revised guides for organ sampling and trimming in rats and mice—part 3: a joint publication of the RITA and NACAD groups. Exp Toxicol Pathol. 55:433–449.

Nadal-Nicolas FM, Jimenez-Lopez M, Sobrado-Calvo P, Nieto-Lopez L, Canovas-Martinez I, Salinas-Navarro M, Vidal-Sanz M, Agudo M. 2009. Brn3a as a marker of retinal ganglion cells: qualitative and quantitative time course studies in naive and optic nerve-injured retinas. Invest Ophthalmol Vis Sci. 50:3860–3868.

Oharazawa H, Igarashi T, Yokota T, Fujii H, Suzuki H, Machide M, Takahashi H, Ohta S, Ohsawa I. 2010. Protection of the retina by rapid diffusion of hydrogen: administration of hydrogen-loaded eye drops in retinal ischemia-reperfusion injury. Invest Ophthalmol Vis Sci. 51:487–492.

Osborne NN, Larsen A, Barnett NL. 1995. Influence of excitatory amino acids and ischemia on rat retinal choline acetyltransferase-containing cells. Invest Ophthalmol Vis Sci. 36:1692–1700.

Osborne NN, Larsen AK. 1996. Antigens associated with specific retinal cells are affected by ischaemia caused by raised intraocular pressure: effect of glutamate antagonists. Neurochem Int. 29:263–270.

Pileri SA, Roncador G, Ceccarelli C, Piccioli M, Briskomatis A, Sabattini E, Ascani S, Santini D, Piccaluga PP, Leone O, et al. 1997. Antigen retrieval techniques in immunohistochemistry: comparison of different methods. J Pathol. 183:116–123.

Presnell JK, Schreibman MP. 1997. Humason's animal tissue techniques. Baltimore, MD: John Hopkins University Press.

Rhodes KJ, Trimmer JS. 2006. Antibodies as valuable neuroscience research tools versus reagents of mass distraction. J Neurosci. 26:8017–8020.

Salinas-Navarro M, Alarcon-Martinez L, Valiente-Soriano FJ, Jimenez-Lopez M, Mayor-Torroglosa S, Aviles-Trigueros M, Villegas-Perez MP, Vidal-Sanz M. 2010. Ocular hypertension impairs optic nerve axonal transport leading to progressive retinal ganglion cell degeneration. Exp Eye Res. 90:168–183.

Sanchez-Migallon MC, Nadal-Nicolas FM, Jimenez-Lopez M, Sobrado-Calvo P, Vidal-Sanz M, Agudo-Barriuso M. 2011. Brain derived neurotrophic factor maintains Brn3a expression in axotomized rat retinal ganglion cells. Exp Eye Res. 92:260–267.

Saper CB. 2005. An open letter to our readers on the use of antibodies. J Comp Neurol. 493:477–478.

Schmeer C, Gamez A, Tausch S, Witte OW, Isenmann S. 2008. Statins modulate heat shock protein expression and enhance retinal ganglion cell survival after transient retinal ischemia/reperfusion in vivo. Invest Ophthalmol Vis Sci. 49:4971–4981.

Shi SR, Imam SA, Young L, Cote RJ, Taylor CR. 1995. Antigen retrieval immunohistochemistry under the influence of pH using monoclonal antibodies. J Histochem Cytochem. 43:193–201.

von Wasielewski R, Mengel M, Gignac S, Wilkens L, Werner M, Georgii A. 1997. Tyramine amplification technique in routine immunohistochemistry. J Histochem Cytochem. 45:1455–1459.

Wassle H, Yamashita M, Greferath U, Grunert U, Muller F. 1991. The rod bipolar cell of the mammalian retina. Vis Neurosci. 7:99–112.

Weishaupt JH, Klocker N, Bahr M. 2005. Axotomy-induced early down-regulation of POU-IV class transcription factors Brn-3a and Brn-3b in retinal ganglion cells. J Mol Neurosci. 26:17–25.

Wen R, Cheng T, Song Y, Matthes MT, Yasumura D, LaVail MM, Steinberg RH. 1998. Continuous exposure to bright light upregulates bFGF and CNTF expression in the rat retina. Curr Eye Res. 17:494–500.

Wen R, Song Y, Cheng T, Matthes MT, Yasumura D, LaVail MM, Steinberg RH. 1995. Injury-induced upregulation of bFGF and CNTF mRNAS in the rat retina. J Neurosci. 15:7377–7385.

WHO, 2001. Neurotoxicity Risk Assessment for human health: principles and approaches—Environmental health criteria S. No. 223. Geneva, Switzerland: World Health Organization.

Xue LP, Lu J, Cao Q, Hu S, Ding P, Ling EA. 2006. Muller glial cells express nestin coupled with glial fibrillary acidic protein in experimentally induced glaucoma in the rat retina. Neuroscience. 139:723–732.

Yamamoto H, Schmidt-Kastner R, Hamasaki DI, Parel JM. 2006. Complex neurodegeneration in retina following moderate ischemia induced by bilateral common carotid artery occlusion in Wistar rats. Exp Eye Res. 82:767–779.